

Constrained-path quantum Monte Carlo simulations of the zero-temperature, disordered two-dimensional Hubbard model

M. Enjalran^{1,4,*}, F. Hébert², G. G. Batrouni², R. T. Scalettar¹, and Shiwei Zhang³

¹ *Physics Department, University of California, Davis, California 95616*

² *Institut Non-Linéaire de Nice, Université de Nice-Sophia Antipolis, 1361, route des Lucioles, 06560 Valbonne, France*

³ *Department of Physics, College of William and Mary, Williamsburg, Virginia 23187.*

⁴ *Materials Research Institute, Lawrence Livermore National Laboratory, Livermore, California 94550.*

(October 25, 2018)

We study the effects of disorder on long-range antiferromagnetic correlations in the half-filled, two dimensional, repulsive Hubbard model at $T = 0$. A mean field approach is first employed to gain a qualitative picture of the physics and to guide our choice for a trial wave function in a constrained path quantum Monte Carlo (CPQMC) method that allows for a more accurate treatment of correlations. Within the mean field calculation, we observe both Anderson and Mott insulating antiferromagnetic phases. There are transitions to a paramagnet only for relatively weak coupling, $U < 2t$ in the case of bond disorder, and $U < 4t$ in the case of on-site disorder. Using ground state CPQMC we demonstrate that this mean field approach significantly overestimates magnetic order. For $U = 4t$, we find a critical bond disorder of $V_c \approx (1.6 \pm 0.4)t$ even though within mean field theory no paramagnetic phase is found for this value of the interaction. In the site disordered case, we find a critical disorder of $V_c \approx (5.0 \pm 0.5)t$ at $U = 4t$. PACS numbers: 74.20.-z, 74.20.Mn, 74.25.Dw

I. INTRODUCTION

The Hubbard Hamiltonian encapsulates many of the most interesting qualitative many-body effects in correlated fermion systems, notably the possibility of ordering of electron spins and the appearance of insulating states in systems with partially filled electronic bands. While the original model is translationally invariant, the introduction of disorder can alter the magnetic and charge correlations in fundamental ways. [1,2] Experimental systems whose qualitative physics appears to involve the interplay of interactions and randomness, possibly modeled by the Hubbard Hamiltonian, include doped semiconductors [2,3], thin superconducting films [4,5], and silicon metal-oxide-semiconductor field-effect transistors. [6]

The determinant quantum Monte Carlo (DQMC) method has been a useful tool to simulate the Hubbard Hamiltonian, [7,8] but its application has been limited by the impossibility of reaching low temperatures in many cases of interest, a problem which arises when the “Boltzmann weight” for the fermion system becomes negative. [8,9] An approach for dealing with this “sign problem” in the ground state is the constrained path quantum Monte Carlo (CPQMC) method. [10] In CPQMC, the sign problem is treated by imposing, in the space of Slater determinants, a boundary condition based on an input trial

wave function.

The CPQMC approach has not previously been used in models with quenched randomness. In this paper, we apply CPQMC to the disordered, two-dimensional (2D), “Anderson-Hubbard” Hamiltonian,

$$\begin{aligned}
 H = & - \sum_{\langle i,j \rangle \sigma} t_{ij} (c_{i\sigma}^\dagger c_{j\sigma} + c_{j\sigma}^\dagger c_{i\sigma}) \\
 & + U \sum_{\mathbf{i}} (n_{i\uparrow} - \frac{1}{2})(n_{i\downarrow} - \frac{1}{2}) \\
 & + \sum_{\mathbf{i}} (\epsilon_{\mathbf{i}} - \mu)(n_{i\uparrow} + n_{i\downarrow}). \quad (1)
 \end{aligned}$$

Here $c_{i\sigma}$ ($c_{i\sigma}^\dagger$) are operators that destroy (create) electrons of spin σ on site \mathbf{i} of a 2D square lattice of size $L^2 = N$. U is the on-site repulsion, μ and $\epsilon_{\mathbf{i}}$ are the chemical potential and random site energies, respectively, and t_{ij} is the (random) hopping energy. Random on-site energies are chosen uniformly on $[-V_s/2, +V_s/2]$, and t_{ij} are chosen uniformly on $[t - V_t/2, t + V_t/2]$, where V_s and V_t are parameters that set the disorder strength. We will choose $t = 1$ to set the scale of energy, and focus our attention on the case when the lattice is half-filled $\langle n \rangle = 1$.

In the absence of disorder, the half-filled Hubbard model has antiferromagnetic (AF) long-range order at all values of the ratio U/t . For large U/t , each site of the lattice is singly occupied, and well defined moments exist. AF order arises as a result of a second-order lowering of energy when neighboring electron spins are antiparallel. In this strong-coupling regime, the density of states $\mathcal{N}(\omega)$ consists of upper and lower Hubbard bands, separated by U . The compressibility $\kappa = N \partial \langle n \rangle / \partial \mu$ vanishes at half-filling, reflecting the presence of a Mott-Hubbard gap.

At weak coupling, AF order is produced by nesting of the Fermi surface, that is, $\epsilon(\mathbf{k} + \mathbf{Q}) = -\epsilon(\mathbf{k})$, at $\mathbf{Q} = (\pi, \pi)$, which results in a divergence of the noninteracting magnetic susceptibility. Here, $\epsilon(\mathbf{k}) = -2t(\cos k_x + \cos k_y)$ is the free-particle dispersion relation in the clean limit. The density of states exhibits a Slater gap at half-filling, arising from this AF order, and again κ vanishes.

Previous DQMC simulations have confirmed this picture of the physics of the clean Hubbard model at half-filling, and made these statements more quantitative. [8,11] An analysis of the effect of bond disorder, which we

shall review below, has also been performed. [12] However, for the case of site disorder, DQMC simulations have not proven possible. In Sec. II, we review the mean field treatment of the problem and consider the effects of disorder in this limit. The CPQMC algorithm is outlined in Sec. III. The effects of disorder on the magnetic correlations are presented in Sec. IV, and we close with a brief summary of our results in Sec. V. The Appendix presents some detailed tests of CPQMC on different model systems (both clean and disordered), with a particular focus on the effect of different choices of the trial wave functions.

II. MEAN FIELD APPROXIMATION

Mean field (MF) theory provides a useful starting point for the analysis of the phase diagram of the Hubbard model and, as we shall see, also provides us with candidate trial wave functions to use in the CPQMC simulations. In this approach, the interaction term is decoupled so that the electrons on site \mathbf{i} of one spin species “see” only the *average* of the density of the other spin species. For zero disorder, the MF phase diagram of the 2D Hubbard model, as a function of filling and U/t , has been given by Hirsch. [13] In the presence of randomness, it is important to consider an unrestricted Hartree-Fock ansatz (UHF) that allows for general site-dependent occupations of each of the two spin species. [14] Systems with electron-phonon interactions with quenched lattice distortions have been studied in this approximation, [15] as have the 3D Anderson-Hubbard model, [16] and the propensity for spontaneous phase separation, stripe formation, and other inhomogeneous charge distributions in the clean Hubbard and related models. [15,17,18,20] One of the purposes of this work is to see how such UHF results compare to those using CPQMC.

We will study the disordered 2D model in the UHF limit, treating bond and site disorder separately. In order to capture the ground state of the model, our calculations are performed at $\beta = 1/T = 100$, where $k_B = 1$. It is useful to define several order parameters for the different possible phases. The magnitude of the z component of the local moment,

$$M_l = \frac{1}{N} \sum_{\mathbf{i}} \langle |m_{\mathbf{i}}| \rangle = \frac{1}{N} \sum_{\mathbf{i}} \langle |n_{\mathbf{i}\uparrow} - n_{\mathbf{i}\downarrow}| \rangle, \quad (2)$$

measures the tendency for sites to have different numbers of up and down spin electrons. The staggered magnetization,

$$M_s = \frac{1}{2N} \sum_{\mathbf{i}} (-1)^{\mathbf{i}} \langle m_{\mathbf{i}} \rangle, \quad (3)$$

determines the degree of long range antiferromagnetic correlation of these moments. Here the notation $\langle \dots \rangle$ represents an averaging over disorder.

It is also useful to look at charge correlations. Two different types of metal-insulator transitions (MIT) can occur in the Anderson-Hubbard model. In the Anderson MIT, the vanishing of the conductivity is driven primarily by the localizing effect of disorder. A useful observable is the inverse participation ratio, R^{-1} ,

$$R^{-1} = \frac{1}{N} \sum_{\mathbf{k}, \sigma, \mathbf{i}} |\psi_{\mathbf{k}\sigma, \mathbf{i}}|^4, \quad (4)$$

where the eigenstates of the Hamiltonian read $|\psi_{\mathbf{k}\sigma}\rangle = \sum_{\mathbf{i}} \psi_{\mathbf{k}\sigma, \mathbf{i}} |\mathbf{i}\sigma\rangle$. For delocalized states, we have $\psi_{\mathbf{k}\sigma, \mathbf{i}} \approx 1/\sqrt{N}$ and $\lim_{N \rightarrow \infty} R^{-1} \rightarrow 0$ in the thermodynamic limit. Meanwhile for localized states, the fermions spread over a few sites and hence R^{-1} goes to a finite value in the thermodynamic limit, signaling localized electrons.

In the Mott MIT, the particles are localized primarily by their interactions. The insulating state is marked by the presence of a gap in the charge spectrum at the Fermi surface and an associated vanishing of the charge compressibility,

$$\kappa = \frac{\partial \langle N_{\text{part}} \rangle}{\partial \mu} = \beta (\langle N_{\text{part}}^2 \rangle - \langle N_{\text{part}} \rangle^2), \quad (5)$$

where N_{part} is the total number of particles in the system, i.e., $N_{\text{part}} = N \langle n \rangle$.

In related work in 3D, [16] M_l has been used to distinguish a “spin-glass-like” and a “paramagnetic” disordered phase that both have $M_s = 0$ but have M_l nonzero and M_l zero, respectively. Interestingly, in two dimensions, we found the very simple result that $M_l = 0$ whenever $M_s = 0$. That is, in a MF treatment of the half-filled two dimensional model it appears that there is no phase in which local moments are present without ordering antiferromagnetically. However, a spin-glass phase has been observed away from half-filling in a similar two dimensional model applicable to the study of $\text{La}_{2-x}\text{Sr}_x\text{CuO}_4$. [21] As we shall comment further below, we are unable to address the possible spin-glass physics with QMC, and so we merely report here that, apparently, within MF theory (MFT) the spin-glass phase is absent in two dimensions. Monte Carlo studies of classical spin glasses have shown that, as with many phase transitions, the appearance of spin-glass order is made less likely as the dimensionality is reduced. [22,23]

A similar difference between two and three dimensions [16] is manifest in the behavior of the inverse participation ratio. We have evaluated R^{-1} but find that it approaches finite values (indicating insulating behavior) throughout the phase diagram of the disordered two dimensional Hubbard model at half-filling. Since R^{-1} is finite and M_l mimics M_s throughout our phase diagram, we will present results only for the staggered magnetization and compressibility.

Figures. 1 and 2 show these observables for sweeps of the disorder strength at fixed values of the interaction. In the case of bond disorder (Fig. 1), the staggered magnetization M_s is nonzero at all but the smallest interactions.

The compressibility, however, has an interesting change in behavior as U increases to $U = 2t$, namely a transition from an Anderson insulating phase with nonzero compressibility to a Mott insulating phase with $\kappa = 0$. [24]

For site disorder there is a much clearer region of vanishing staggered magnetization and hence paramagnetic behavior. At $U = 2t$, for example, M_s vanishes beyond $V_s = 4t$. At $U = 4t$, however, the physics becomes rather similar to the bond disordered case, with AF correlation extending to very large values of disorder, and a signature of a Mott transition in the compressibility. The enlargement of the paramagnetic phase space at the expense of the antiferromagnetically ordered Mott and Anderson phases is presumably a consequence of the existence, with site disorder, of potential wells on which pairs can form, destroying the moments. Similarly, we observe that on-site disorder is more effective at eliminating the charge gap than bond disorder.

We used these, and other, sweeps of disorder strength at fixed interaction to generate the full UHF ground state phase diagrams of the site- and bond-disordered two dimensional Hubbard models as shown in Figs. 3 and 4. We observed both antiferromagnetically ordered Anderson and Mott insulating phases, and a paramagnetic Anderson insulating region. These three phases are described by

- Paramagnetic Anderson insulator (P AI): $M_l = 0$, $M_s = 0$, $\kappa \neq 0$, $R^{-1} \neq 0$.
- Antiferromagnetic Anderson insulator (AF AI): $M_l \neq 0$, $M_s \neq 0$, $\kappa \neq 0$, $R^{-1} \neq 0$.
- Antiferromagnetic Mott insulator (AF MI): $M_l \neq 0$, $M_s \neq 0$, $\kappa = 0$, $R^{-1} \neq 0$.

In the case of bond disorder, systems of size 6×6 , 8×8 , and 10×10 were simulated with averages from 40, 50, and 50 disorder realizations, respectively. AF order dominates the MF phase diagram, as might be expected since the disorder is not destroying the moments directly, and MFT is too primitive to pick up subtle effects such as destruction of AF order via singlet formation. The paramagnetic region is restricted to a narrow wedge with $V_t > 16U$. For $U > 2t = W/4$ (where W is the bandwidth of the 2D tight binding model) we observe AF ordered phases both of the Mott and Anderson variety with a boundary given roughly by $U = 2t + V_t/4$. For $U < 2t = W/4$ there is no Mott gap within MFT.

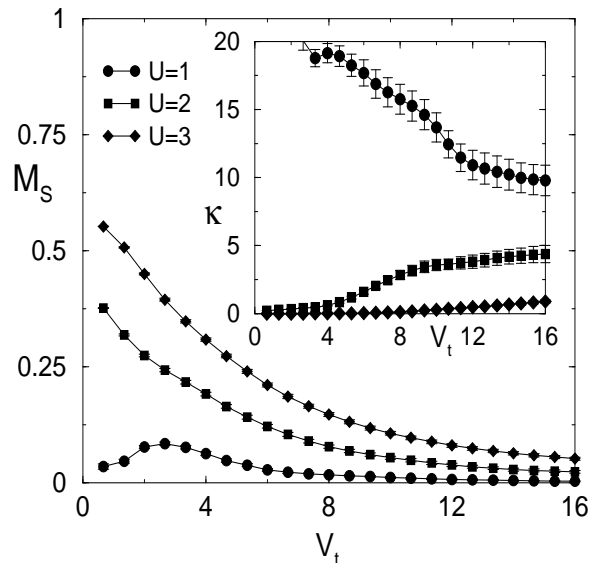


FIG. 1. Staggered magnetization and compressibility for the case of bond disorder on a 10×10 lattice in the unrestricted Hartree-Fock approximation. AF long-range order (LRO) is destroyed by bond disorder for weak on-site interactions, $U \lesssim 1.0$. The staggered magnetization, M_s , levels off in the thermodynamic limit for $U \gtrsim 2.0$, and no amount of disorder destroys AF LRO. The inset shows the behavior of the compressibility with V_t . A gap is present at $U > 2.0$ and $V_t < 2.0$, but it is destroyed with increasing disorder.

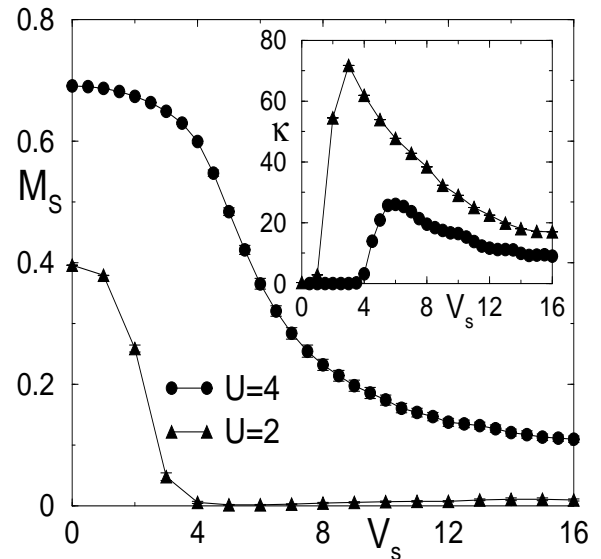


FIG. 2. Evolution of the staggered magnetization and compressibility for on-site disorder on a 12×12 lattice. While there is a transition to a paramagnetic state for $U = 2$, the system remains antiferromagnetic even at large V_s for $U = 4$. The compressibility (inset) indicates that the presence of a gap is more sensitive to site disorder than to bond disorder.

In the case of site disorder, the antiferromagnetic Mott insulator exists for interaction strengths that obey $U >$

V_s . When $U > 2t$ the antiferromagnetic Mott insulator is first supplanted by an antiferromagnetic Anderson insulator with increasing disorder and then ultimately by a paramagnetic Anderson insulator at much larger V_s . For $U < 2t$ the transition from antiferromagnetic Mott insulator appears to go directly to the paramagnetic Anderson insulator.

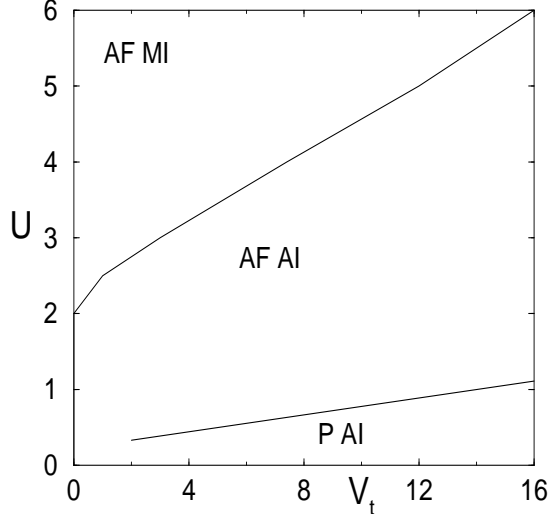


FIG. 3. Phase diagram of the bond-disordered Hubbard model within the unrestricted Hartree-Fock limit. P = paramagnet, AF = antiferromagnet, AI = Anderson insulator, MI = Mott insulator.

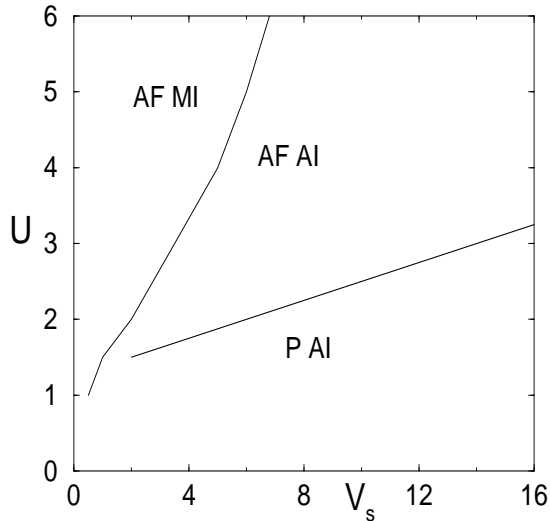


FIG. 4. Phase diagram of the site-disordered Hubbard model within the unrestricted Hartree-Fock limit. P = paramagnet, AF = antiferromagnet, AI = Anderson insulator, MI = Mott insulator.

In summary, a few notable results from our mean field calculation are the following: (i) The same three phases, AF ordered Mott insulator, AF ordered Anderson insulator, and paramagnetic Anderson insulator, are observed

for bond and site disorder. (ii) We saw no evidence for metallic ($R^{-1} = 0$) or spin-glass-like ($M_l \neq 0$ with $M_s = 0$) behavior. (iii) AF LRO is never destroyed by disorder even at relatively modest values of the interaction, e.g., $U \gtrsim 2t$ for bond disorder and $U \gtrsim 4t$ for site disorder.

III. DESCRIPTION OF THE CPQMC SIMULATION

The ground-state CPQMC method was developed to study correlated lattice electrons where no special particle-hole symmetry exists to eliminate the sign problem. It applies techniques that are a hybrid of determinant Quantum Monte Carlo [7] (DQMC) and diffusion Monte Carlo [25] (DMC) methods.

Like the DQMC technique, the method employs the Hubbard-Stratonovich (HS) transformation to decouple the interaction term of the Hamiltonian, $U \sum_i n_{i\uparrow} n_{i\downarrow}$. The result is a quadratic Hamiltonian in which the interaction between electrons has been replaced by the interaction of independent electrons with a classical fluctuating field. Sampling over the possible values of the HS field reproduces the original electron-electron interaction.

This quadratic Hamiltonian can then be used in an imaginary time propagation of a Slater determinant, allowing projection of the ground state from an initial trial wave function: $|\psi_0\rangle = \lim_{\tau \rightarrow \infty} \exp(-\tau H)|\psi^{(o)}\rangle$. The similarity to the DMC method comes from the fact that the imaginary time propagation is represented by an ensemble of random walkers. (However, the random walk in the CPQMC method is performed in a space of Slater determinants, in contrast to the DMC method where the random walk is in configuration space.) The constrained path approximation, necessary for dealing with negative weights, is similar in spirit to the fixed node [26] approximation commonly used to study correlated fermions in the continuum. It imposes a boundary condition in determinant space with a trial wave function, which constrains the random walkers to half of the over-complete determinant space. The details of the CPQMC algorithm have been discussed elsewhere [10], but we will provide a brief description followed by a discussion of the necessary adjustments to treat disorder and the observables of interest.

A. Generation of configurations

At any time in the CPQMC simulation, the wave function is represented by an ensemble of random walkers. More specifically, we work in a single Slater determinant basis and represent our wave function at imaginary time step n by $|\psi^{(n)}\rangle \propto \sum_k |\phi_k^{(n)}\rangle$, where $|\phi_k^{(n)}\rangle$ is an individual walker (Slater determinant). The initial wave function $|\psi^{(o)}\rangle$ can in principle be any linear combination of Slater

determinants not orthogonal to the ground state. For convenience, we choose it to be the unrestricted Hartree-Fock wave functions discussed earlier, i.e., $|\psi^{(0)}\rangle \equiv |\psi_T\rangle$.

In order to propagate the wave function forward to imaginary time τ , we discretize the propagator to a series of short time steps, $\Delta\tau$. This allows us to apply the Trotter approximation

$$\exp(-\Delta\tau H) = \exp(-\frac{\Delta\tau K}{2}) \exp(-\Delta\tau W) \exp(-\frac{\Delta\tau K}{2}),$$

and isolate the potential energy W from the kinetic energy K . The HS transformation is then applied,

$$\exp(-\Delta\tau U n_{i\uparrow} n_{i\downarrow}) = \exp\left(-\frac{\Delta\tau U (n_{i\uparrow} + n_{i\downarrow})}{2}\right) \sum_{x_i=\pm 1} p(x_i) \exp[\gamma x_i (n_{i\uparrow} - n_{i\downarrow})], \quad (6)$$

where $\cosh(\gamma) = \exp(\Delta\tau U/2)$, $p(x_i) = 1/2$, and x_i is the HS field at site i . At each imaginary time step the interaction part of the propagator is now a function of the HS field.

Because of the special form of the propagator, each Slater determinant $|\phi_k^{(n)}\rangle$ in the representation of the wave function at imaginary time step n is transformed into another Slater determinant $|\phi_k^{(n+1)}\rangle$ at imaginary time step $n+1$. We thereby apply the incremental projection operator repeatedly to the wave function of our system to project out the ground state. In order to make the sampling more efficient we can employ an importance function to modify the original probability distribution, as has been discussed. [10] As in the DQMC algorithm, the computation time in the CPQMC algorithm scales roughly as $N^3 N_w$ per random walk step, where N is the number of spatial sites in the lattice and N_w is the number of walkers.

The CPQMC algorithm is exact up to this point. A remaining issue is the constraint to deal with the sign problem, which is usually implemented with the importance function. We define the overlap integral $O_T \equiv \langle \psi_T | \phi_k \rangle$, and demand that individual walkers maintain a positive O_T , i.e., that they do not cross the boundary $\langle \psi_T | \phi_k \rangle = 0$ in their random walk in Slater determinant space. This is applied to every walker at every time step. The constraint is an approximation, whose quality depends on the quality of the trial wave function $|\psi_T\rangle$.

B. Measurements

Monte Carlo methods such as the CPQMC technique that employ trial wave functions are well suited for calculating the ground-state energy, and initial work on the CPQMC method [10] demonstrated an excellent agreement of the ground state energy with exact approaches in cases where exact results were available. [27] In the Appendix, we will demonstrate that this agreement, though a bit less accurate, extends to our simulations.

In the body of the paper, however, we will focus on real space magnetic order which can be identified by measuring the correlation function,

$$C(\mathbf{l}) = \frac{1}{N} \sum_{\mathbf{j}} \langle m_{\mathbf{j}} m_{\mathbf{j}+\mathbf{l}} \rangle. \quad (7)$$

Here $m_{\mathbf{j}} = n_{\mathbf{j}\uparrow} - n_{\mathbf{j}\downarrow}$ is the z component of the local spin operator, and N is the total number of lattice sites. $C(0,0)$ measures the squared local magnetic moment $\langle m_{\mathbf{j}}^2 \rangle$. In the clean system, $C(0,0) = 0.5$ in the noninteracting limit, and saturates at $C(0,0) = 1$, as U is increased. In the clean system, $\langle m_{\mathbf{j}} m_{\mathbf{j}+\mathbf{l}} \rangle$ is translationally invariant, that is, independent of \mathbf{j} . For a particular disorder realization, however, this is not the case, and translational invariance is restored only after disorder averaging.

It is useful to consider the magnetic structure factor, the Fourier transformation of $C(\mathbf{l})$,

$$S(\mathbf{q}) = \sum_{\mathbf{l}} C(\mathbf{l}) e^{i\mathbf{q}\cdot\mathbf{l}}. \quad (8)$$

The structure factor will have sharp peaks at ordering vector \mathbf{Q} when long-range magnetic order is present. $\beta S(0,0)$ is the uniform spin susceptibility. At half-filling, we always find $S(\mathbf{q})$ to be largest at the commensurate vector $\mathbf{Q} = (\pi, \pi)$, even in the presence of randomness. However, our resolution in momentum space is rather coarse and ordering at \mathbf{Q} values close to (π, π) would be difficult to see unless the lattice sizes were much increased.

For finite lattice simulations, the issue of the presence of long-range order in the thermodynamic limit may be settled by examining the scaling properties on lattices of different size. Spin wave theory [28] predicts

$$C(L/2, L/2) = \frac{M_s^2}{3} + O(L^{-1}),$$

$$\frac{S(\pi, \pi)}{N} = \frac{M_s^2}{3} + O(L^{-1}). \quad (9)$$

Here M_s is the sublattice magnetization in the thermodynamic limit, and $(L/2, L/2)$ is the maximal separation on a square lattice of linear size $L = \sqrt{N}$ with periodic boundary conditions. C and S provide two quantities to extrapolate the value of the ground state order parameter.

It is important to comment on the differences of behavior between the order parameters based on local moments such as M_l and M_s [Eqs. 2 and 3], which one might expect to find in comparing mean field and QMC treatments. First, because of the relatively modest spatial lattice sizes being simulated in the QMC scheme, over the course of a typical run the simulation is able to explore the equivalent states that have a surplus of up-spin electrons and a surplus of down-spin electrons on a given site. In the thermodynamic limit, like a real material,

the simulation could get stuck in one or the other, but our lattice sizes are not large enough for that to happen. As a consequence, any direct measurement we make of M_s always vanishes, and M_s can only be inferred from the finite size scaling analysis, Eq. 9. Meanwhile, MFT is able to study M_s directly. Second, MFT has a well-known tendency to over-estimate the sharpness of the behavior of the local moment as a function of the ratio of interaction strength to band-width. For example, even in the clean system, phase transitions associated with magnetic long-range order are often associated also with abrupt formation of local moments. However, it is well established that within the QMC method the evolution of the local moment is much less abrupt. [8] For both these reasons, we do not expect to be able to observe any spin-glass (SG) phase transition within the QMC method, nor indeed do we see one. In this work we are only able to report that the SG transition observed in MFT at half-filling in the three-dimensional model apparently does not occur within the same MF treatment in two dimensions. Spin-glass order in interacting Fermi systems has generated much interest recently, but most investigations have relied on field theoretic and renormalization-group-type techniques. [29]

The effect of disorder on the size or existence of the Mott gap in the CPQMC method is an interesting question that will not be considered in detail in this work. We have measured the density as a function of chemical potential [30] and the compressibility, and find the Mott gap is rather strongly reduced by site disorder and considerably less affected by bond disorder, [31] but we leave a detailed analysis to a later presentation.

IV. RESULTS FOR MAGNETIC CORRELATIONS

In this section we address the primary point of interest in the paper, the effect disorder has on the long-range magnetic order of the half-filled 2D Hubbard model. In particular, we want to determine the critical disorder strength necessary to destroy the magnetically ordered ground state and ascertain the accuracy of the UHF phase diagram. We concentrate on the case where $U = 4t$, where the UHF shows no transition to a paramagnetic order. This antiferromagnetic to paramagnetic transition can only take place in the thermodynamic limit; hence we resort to finite size scaling techniques to calculate the disorder strength at which AF LRO is lost. In the case of bond disorder, these questions have been investigated previously with the DQMC method since there is no sign problem. [12] We re-address these questions here in order to benchmark the accuracy of the CPQMC method. After the results for bond disorder are discussed, we consider the case of random site energies and its ability to drive the model from an antiferromagnet to a paramagnet. We again point out that the site-disordered problem has not yet been studied with the QMC

method because of the sign problem.

A. Bond disorder

The mechanism by which bond disorder destroys AF LRO is the formation of spin-0 singlets. When the disorder becomes large, the lattice contains strong bonds where it is favorable for nearest neighbors to form singlets rather than participate in AF LRO. Unlike the case of site disorder, one would expect the persistence of local correlations, $C(0, 0)$, even in the paramagnetic phase.

In our simulations of this problem, we draw random near-neighbor hopping strengths from a uniform distribution about a mean value of $\langle t_{ij} \rangle = t = 1$, e.g., $[1 - V_t/2, 1 + V_t/2]$. We considered simulations with a renormalized interaction, $U_{\text{CPQMC}} \neq U$, chosen, as described in the Appendix, so the CPQMC and DQMC results match in the clean limit. For 4×4 , 6×6 , and 8×8 lattices the values of U_{CPQMC} were set to 1.25, 1.75, and 1.85, respectively. Disorder averaging was performed on 10 realizations for each disorder strength on each lattice. We used as $|\psi_T\rangle$ an UHF trial wave function (TWF) obtained with $U_{\text{TWF}} = 2$, but as shown in the Appendix, the results are not sensitive to this choice. [32]

The real space spin correlations are shown in Fig. 5 on a fixed 8×8 lattice size. Disorder substantially decreases the antiferromagnetic order, with only a relatively minor suppression of the squared local moment (inset).

Summing up these real space spin correlations yields the magnetic structure factor. Working on a range of lattice sizes, and employing the scaling relationship for $S(\pi, \pi)$, Eq. 9, yields the staggered magnetization as a function of disorder from the intercepts of our scaling plot, Fig. 6.

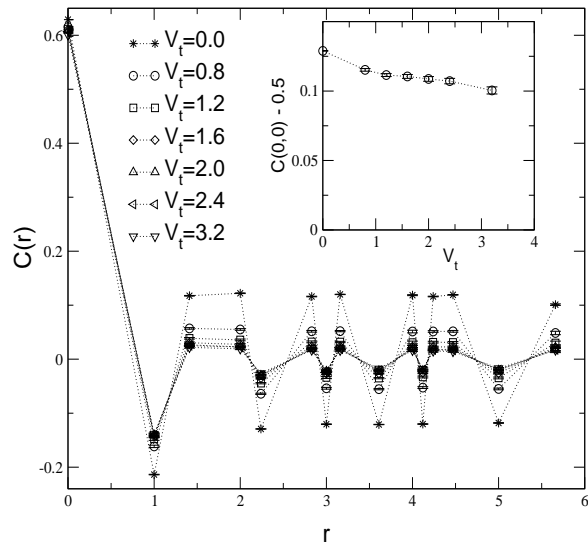


FIG. 5. The real space spin-spin correlations on a bond-disordered 8×8 lattice. The inset shows the squared local moment scaled by the noninteracting value as a function of bond disorder strength.

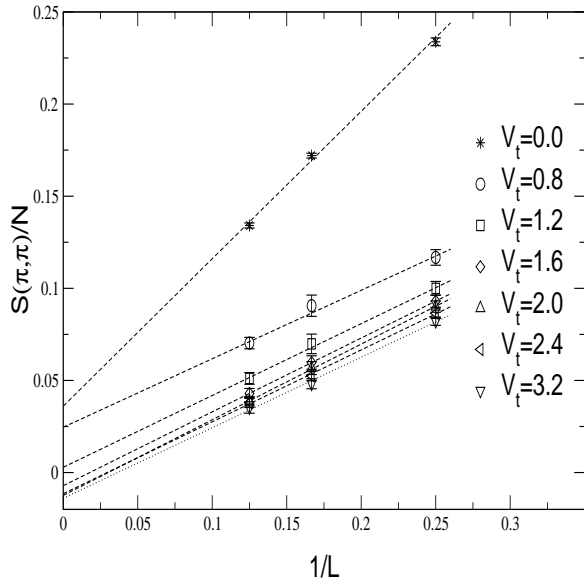


FIG. 6. Finite size scaling for the structure factor as a function of bond disorder. Simulations were performed with a renormalized interaction and an UHF trial state with $U_{\text{TWF}} = 2$. Extrapolations to the thermodynamic limit give an intercept that is equal to $M_s^2/3$. A critical disorder strength of $V_t \approx 1.6 \pm 0.4$ is found, which agrees with the DQMC result. The dashed lines are linear least squares fits to the data.

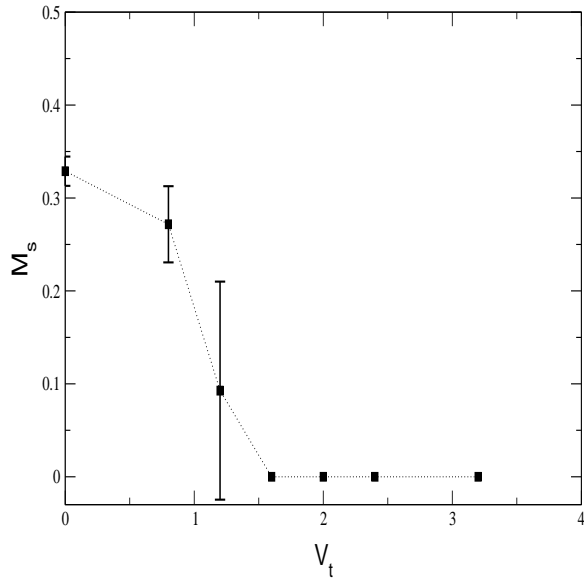


FIG. 7. Staggered magnetization as a function of bond disorder. Values were calculated from the intercepts of Fig. 6. M_s vanishes at the critical disorder strength $V_t \approx 1.6 \pm 0.4$.

It is worth making two further comments concerning Fig. 6. First, in papers establishing long-range antiferromagnetic order in the clean, half-filled, two-dimensional Hubbard model, extrapolations of both the longest-range spin-spin correlation function $C(L/2, L/2)$ and the struc-

ture factor $S(\pi, \pi)$ were done. [8] The error bars on C were only slightly larger than those from S , so they provided essentially equivalent (and consistent) information. In the disordered system, however, we have found that C is not as useful to examine as the structure factor. We believe that the reason is that on a lattice of N sites, C is obtained through an average over only the $O(N)$ pairs of sites separated by $(L/2, L/2)$ while S involves all $O(N^2)$ separations. The structure factor is thus much less sensitive to individual disorder realizations. Second, the linear extrapolation to negative order parameter in the disordered phase evident in Fig. 6 has been observed in previous simulations, e.g., of the clean periodic Anderson model as the hybridization between localized and delocalized orbitals is increased until the antiferromagnetism gives way to Kondo singlet formation. [33] The point is that Eq. 9, which yields a linear extrapolation in $1/L$, is valid only in the ordered phase. In the disordered phase $S/N \propto b/L^2$ so one should actually fit the data to a quadratic expression that goes through the origin.

The results for M_s are exhibited in Fig. 7, which gives a critical disorder of $V_t = 1.6 \pm 0.4$. The UHF calculation predicts no transition to a paramagnetic phase for this value of U , but the CPQMC calculation agrees very well with the previous DQMC results. [12] We did not observe an enhancement of M_s at weak disorder as was observed in our UHF data and in DMFT and DQMC calculations, [31,12] but our resolution might be too small to observe this effect.

B. Site disorder

In our simulations of the site-disordered model, random energies were selected from a uniform distribution $\epsilon_i \in [-V_s/2, V_s/2]$. Sites with $\epsilon_i < 0$ favor double occupancy while sites with $\epsilon_i > 0$ favor the unoccupied state. This leads to a direct destruction of moments, unlike the case of bond disorder. In the presence of a repulsive Hubbard interaction U , there is therefore a competition between a lattice with local moments and AF LRO, which is favored by U , and a state of doubly occupied and empty sites favored by the disorder.

As discussed in the Appendix, simulations with on-site disorder need to have $U_{\text{TWF}} > V_s$ in order to capture the physics of the model and not the effect of trial wave function. We used a trial wave function with $U_{\text{TWF}} = 6$, and the same renormalized interaction U_{CPQMC} used in the bond-disordered case. We simulated 10 realizations of each disorder strength. The suppression of the real space spin correlations is displayed in Fig. 8.

We can again analyze appropriately scaled data on different lattices, with the results shown in Fig. 9. The intercepts give the staggered magnetization, which is driven to zero above a critical site disorder strength of $V_s \approx 5.0 \pm 0.5$ (Fig. 10). The UHF calculation predicts no transition to a paramagnetic phase for this value of U .

Hence, our UHF trial wave function has long-range antiferromagnetic correlations throughout the range of V_s in Fig. 10, and the destruction of order is not associated with any change in the nature of $|\psi_T\rangle$.

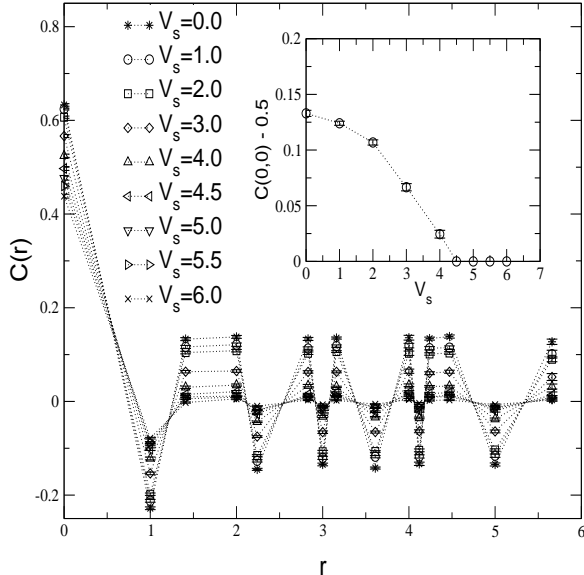


FIG. 8. The effect of site disorder on the real space spin-spin correlations on an 8×8 lattice. Correlations for distances greater than 1 are uniformly reduced by disorder. The inset shows the behavior of the scaled squared local moment as a function of V_s . Site disorder strongly suppresses the local moment.

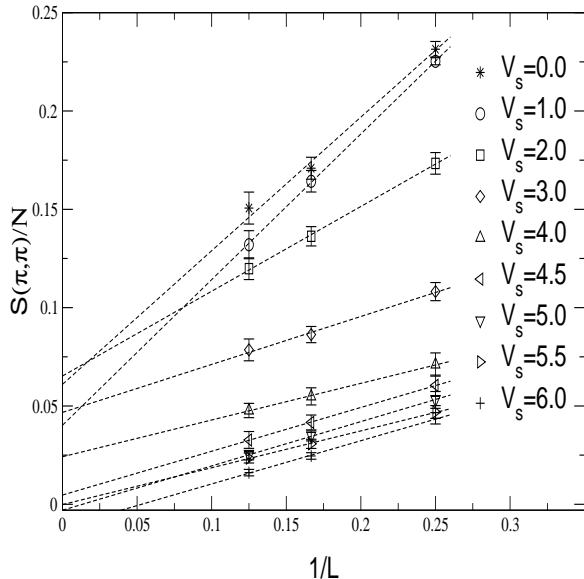


FIG. 9. Scaling relationship for the site disordered model with a renormalized U_{CPQMC} and an UHF trial state with $U_{\text{TWF}} = 6$. The critical disorder strength was $V_s \approx 5.0 \pm 0.5$. The dashed lines are linear least-squares fits to the data.

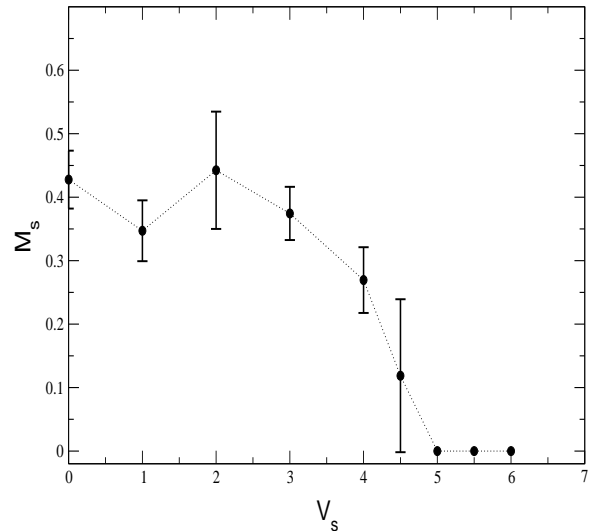


FIG. 10. Staggered magnetization (M_s) for the site-disordered 2D Hubbard model. Data were obtained from the intercepts of the scaling relationship for $S(\pi, \pi)$, Fig. 9. M_s vanishes at $V_s \approx 5.0 \pm 0.5$.

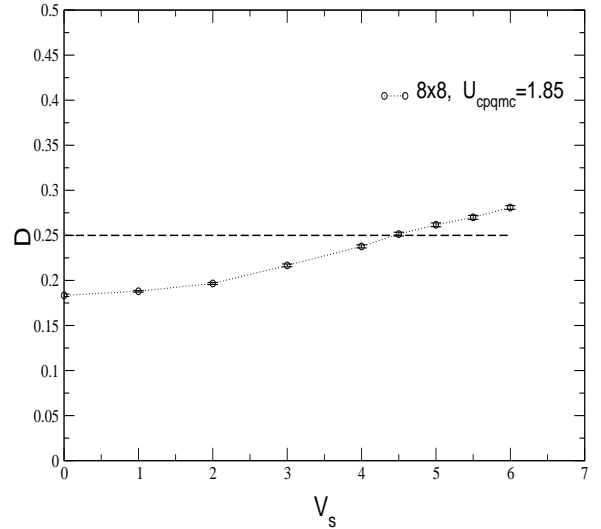


FIG. 11. The double occupancy as a function of site disorder on an 8×8 lattice. The dashed line denotes the separation between the repulsive (below) and attractive (above) Hubbard model at $t = 0$ and any temperature. Data were obtained from simulations with $U_{\text{CPQMC}} = 1.85$ and $U_{\text{TWF}} = 6$.

It is interesting that the point at which AF LRO is lost corresponds rather closely to the value of randomness where the squared local moment is reduced below its noninteracting value. This is emphasized in Fig. 11, which shows the average double occupancy $D = \langle n_{\uparrow} n_{\downarrow} \rangle = E_I / U_{\text{CPQMC}}$ in the CPQMC method, where E_I is the interaction energy of the fermions. Since $C(0, 0) = 1 - 2D$, an enhancement of D above the noninteracting value is synonymous with the moment falling below the $U = 0$ value.

V. CONCLUSIONS

We have studied the ground state half-filled 2D Hubbard model with both bond and site disorder in the mean field limit and by the constrained path quantum Monte Carlo method. Our most significant quantitative result was the first computation of the critical disorder strength for the destruction of antiferromagnetic long-range order by site randomness, $(V_s)_{\text{crit}} = 5t$ for $U = 4t$. For this value of the interaction strength, no amount of site disorder destroys the order in the Hartree-Fock approach, so this emphasizes the need for better treatment of correlations that techniques like the quantum Monte Carlo method provide. In general, we find that UHF calculations grossly overestimate the tendency for magnetic order when compared to the CPQMC calculations, as might be expected by an approach which ignores fluctuations.

There is less significant disagreement between UHF and CPQMC techniques for the transport properties. Unlike the 3D case, the UHF treatment finds that the 2D Hubbard model is insulating for all values of interaction and disorder at half-filling: the inverse participation ratio was always nonzero. This is consistent with recent QMC calculations in two dimensions. [34] A further difference between the 2D and 3D UHF results is our conclusion that the spin-glass phase is absent in two dimensions at half-filling. It is interesting to note that there have been some indications in the QMC treatment of a metal-insulator transition *off half-filling* in the 2D Hubbard model. [35]

Our work further evaluated and extended the range of validity of the CPQMC method by applying it to random systems. We found that, as is the case for clean systems, the CPQMC technique can provide an accurate way of treating the Hubbard model. In particular, it gives the same critical disorder strength as the DQMC method in the case when DQMC has no sign problem (bond randomness), which provides some confidence in applying it to cases such as site-disordered problems where the DQMC method cannot give reliable results.

Much of the initial theoretical evidence for, and understanding of, questions of charge ordering in Hubbard-like models has come from UHF treatments. [18] Recent work with techniques such as the density matrix renormalization group have emphasized that stripe formation is a subtle and delicate effect. [19] Our work indicates that there are significant corrections to the spin correlations within UHF treatments, and that further CPQMC calculations hold promise to shed some light on the behavior of disordered and interacting electron systems.

ACKNOWLEDGMENTS

We would like to thank Malvin Kalos for many useful discussions. M. E. would also like to acknowledge the

support of the Material Research Institute at Lawrence Livermore National Laboratory and the Institut Non-Linéaire de Nice-Sophia Antipolis, Valbonne, France for their hospitality during a visit where valuable work on this collaboration was conducted. This work was supported by the Materials Research Institute of LLNL, by NSF-DMR-9985978, and also by NSF-DMR-9734041. S. Z. is a Research Corporation Cottrell Scholar. Work at Lawrence Livermore National Laboratory performed under the auspices of the U.S. Department of Energy under contract No.: W-7405-ENG-48.

APPENDIX: TESTS OF THE ALGORITHM

In this Appendix we describe some tests of the CPQMC algorithm with a specific focus on the effect of the trial wave functions on the results. Previously, the CPQMC algorithm has been extensively tested for interacting systems with no disorder. Investigations have been performed on the single-band Hubbard model in regions of parameter space where a severe sign problem is known to exist. [10] The method has also been used to study superconductivity in the 2D Hubbard model by looking for long-range pairing correlations in the ground state [36] and for ferromagnetism in the periodic Anderson model. [37] Here disorder has been considered within a CPQMC calculation.

CPQMC is an exact algorithm, for all observables, in the absence of interactions, even when disorder is turned on. As a check of our code, we therefore first verified that the CPQMC code reproduced results from exact diagonalization (ED) at different disorder strengths. Likewise, the DQMC algorithm agrees perfectly with ED results. [38]

We next looked in detail at the behavior of the magnetic structure factor as a function of disorder and interaction strengths, and as a function of the trial wave function. In the following discussion it is useful to distinguish between the value of the interaction strength, U_{CPQMC} , used in the CPQMC algorithm, the value of the interaction strength, U_{TWF} , used in the trial wave function, and the physical value of U in the Hamiltonian. We concentrate here on the case where $U = 4t$ and $t = 1$. In our DQMC simulations, which we used to provide benchmarks for the CPQMC method, we of course always choose $U_{\text{DQMC}} = U$ since the DQMC treatment is exact. [38]

The key result of our studies is that the CPQMC technique with UHF trial wave functions significantly overestimates the magnetic correlations if $U_{\text{CPQMC}} = U$. This is illustrated in Fig. 12, which shows the ratio of the CPQMC to DQMC structure factors for the clean system on a 4×4 lattice as a function of U_{CPQMC}/U . The results are independent of the value of U_{TWF} as long as $U_{\text{TWF}} \neq 0$. The structure factor is the same for the two methods when $U_{\text{CPQMC}}/U \approx 0.31$ or $U_{\text{CPQMC}} \approx 1.25$. For 6×6 and 8×8 lattices agreement is attained at

$U_{\text{CPQMC}} \approx 1.75$ and $U_{\text{CPQMC}} \approx 1.85$, respectively, for $U = 4$.

4x4 lattice, half-filled, $U_{\text{dqmc}}=4$ $V_s=0.01$

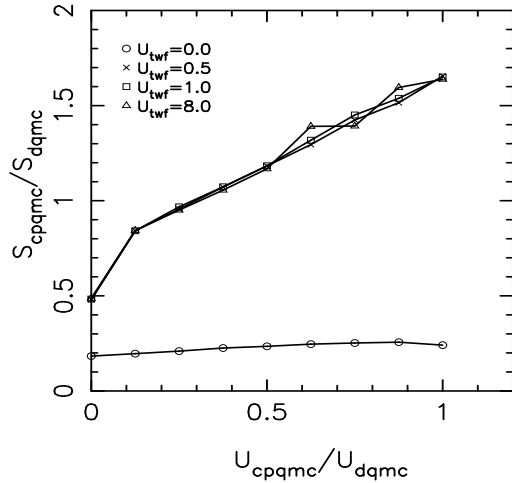


FIG. 12. Scaled data for $S(\pi, \pi)_{\text{CPQMC}}/S(\pi, \pi)_{\text{DQMC}}$ as a function of $U_{\text{CPQMC}}/U_{\text{DQMC}}$ for the clean Hubbard model in the CPQMC treatment. When $U_{\text{CPQMC}} = U_{\text{DQMC}} (= U)$, AF LRO is considerably overestimated. We found agreement between the two methods at $U_{\text{CPQMC}} \approx 1.25$ for this 4×4 lattice. The interaction strength U_{TWF} of the UHF trial wave function does not affect results as long as $U_{\text{TWF}} \neq 0$.

A similar effect is seen when disorder is turned on, as illustrated in Fig. 13 for site disorder. Here we show the ratio of the CPQMC and DQMC structure factors as a function of U_{CPQMC}/U for different lattice sizes. These results are for a single realization of disorder, which is kept fixed as U_{CPQMC} and U_{TWF} are varied. The values of the CPQMC structure factor for different U_{TWF} fall onto two curves: For all $U_{\text{TWF}} > V_s$, the CPQMC method gives the same significantly overestimated structure factor. Meanwhile, for all $U_{\text{TWF}} < V_s$, the CPQMC methods gives the same significantly underestimated structure factor.

These different behaviors are a direct manifestation of the trial wave functions. In the unrestricted Hartree-Fock calculation, both U_{TWF} and V_s act as one-body potentials and compete with each other: When $U_{\text{TWF}} < V_s$, V_s dominates and double occupancy is allowed, i.e., the system is more free-electron like; when $U_{\text{TWF}} > V_s$, U_{TWF} dominates, double occupancy is discouraged, and the system prefers to be in an AF state. Clearly, the CPQMC technique could not adequately eliminate the biases that the two different classes of UHF trial wave functions introduce through the approximate constraint to bring quantitative agreement between the two sets of results. In all the work reported in the body of this paper we chose $U_{\text{TWF}} > V_s$ so that the trial wave function had long-range antiferromagnetic order. The destruction of order as randomness increased therefore must occur from correlation effects and not from any transition in the trial

wave function.

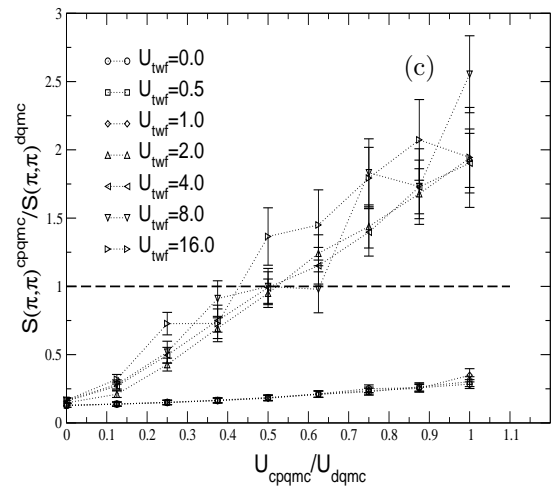
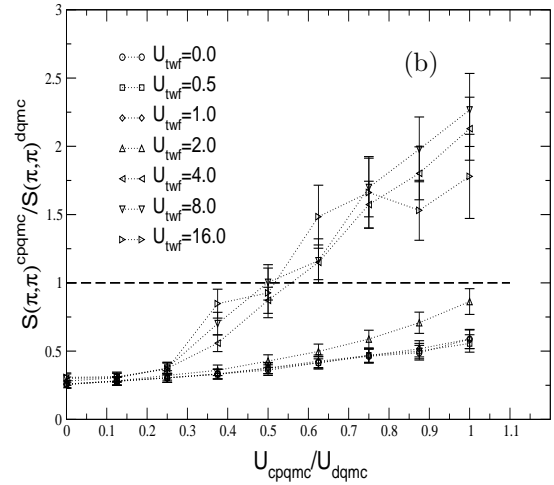
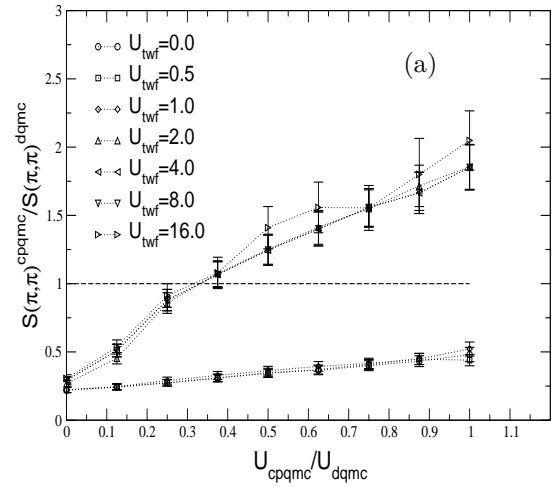


FIG. 13. Scaled data for $S(\pi, \pi)_{\text{CPQMC}}/S(\pi, \pi)_{\text{DQMC}}$ for the site-disordered Hubbard model in the CPQMC technique: (a) 4×4 , $V_s = 2$; (b) 4×4 , $V_s = 4$; (c) 6×6 , $V_s = 2$.

Bond disorder is studied in Fig. 14. The CPQMC structure factor is again overestimated. Bond disorder V_t , however, does not turn into one-body potentials in the UHF method in a simple manner, and unlike site disorder, there are not two separate behaviors. The result is rather independent of U_{TWF} . [32]

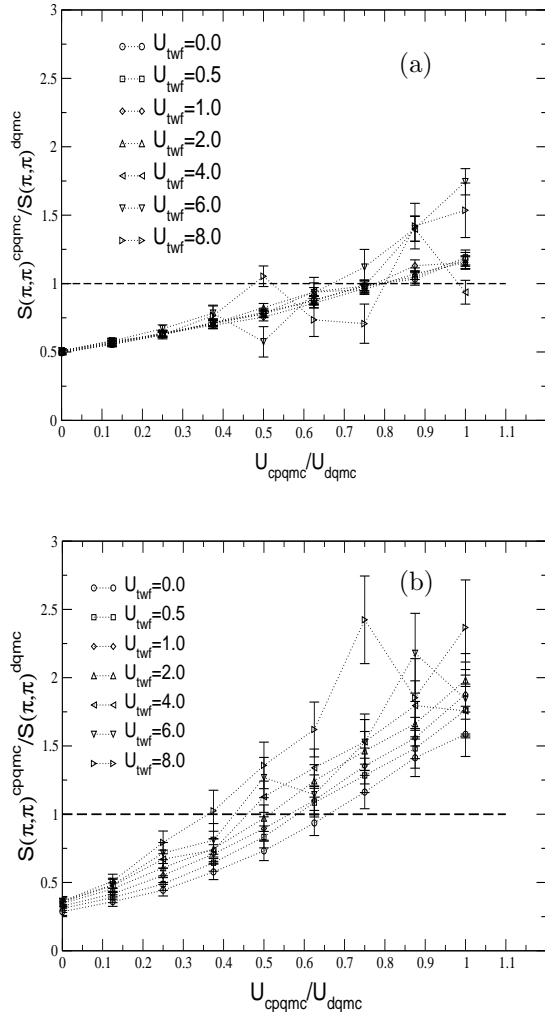


FIG. 14. Scaled data for $S(\pi, \pi)_{\text{CPQMC}}/S(\pi, \pi)_{\text{DQMC}}$ for the bond-disordered Hubbard model in the CPQMC method: (a) 4×4 , $V_t = 2$; (b) 6×6 , $V_t = 2$.

While we show results for single disorder realizations in Figs. 13 and 14, the values of the renormalized couplings used in determining, for example, the critical disorder strength, in the main text of this paper were obtained with disorder averaging. The overestimation of the structure factor is a significant concern in our studies of the destruction of long-range antiferromagnetic order, which rely primarily on this quantity. It exemplifies the difficulty that faces all approximate methods to deal with the sign problem that use a trial wave function to constrain the QMC sampling, namely the results can be biased by the trial wave function, sometimes significantly. Our ap-

proach is to fix U_{CPQMC} at a “renormalized” value so that the structure factor from the CPQMC algorithm matches the DQMC result. This sort of tuning of the interaction strength has previously been done in comparisons of diagrammatic calculations for the Hubbard model with DQMC results. [39] A crucial question, of course, is whether the renormalized U_{CPQMC} is independent of lattice size. We found that U_{CPQMC} depends only weakly on lattice size for $L > 4$, as seen in Fig. 14. Again, similar effects are known in the comparisons of DQMC and diagrammatic calculations. [39]

A further indication of the importance of the renormalization of the interaction lies in the behavior of the staggered magnetization per site. Data using a renormalized U_{CPQMC} always lie below the classical upper limit of 0.5 whereas simulations for fixed $U_{\text{CPQMC}} = U$ did not. At $V_t = 0$, our result with a renormalized U_{CPQMC} and $U_{\text{TWF}} = 2$ was $M_s = 0.33(2)$. This clean system value compares well to earlier results for the quantum Heisenberg model obtained from a QMC calculation, 0.30(2), [40] and from perturbation series expansions, 0.313. [28]

Another crucial question is whether the renormalized U_{CPQMC} depends on disorder strength. This question can be addressed in the case of bond disorder where DQMC simulations of large lattices at low T can be done without encountering the sign problem, but cannot be done for site disorder. We found that for a given lattice size a single constant choice of U_{CPQMC} could be used for all V_t . [32] We note that the apparent variation of the renormalization on the values of V_s and V_t evident in comparing Figs. 12–14 is dominantly due to the fact the data presented there are not disorder averaged, a particularly important issue for the smaller 4×4 lattices. When such averaging is done, as in the main body of this paper, the variation is very significantly reduced. This is fortunate, since the tuning of U_{CPQMC} for different disorder strength would be not only awkward but would also call into question whether transitions we observe as a function of disorder strength were caused by the tuning or by the randomness itself.

We have focused here on the behavior of the structure factor and matching the DQMC and CPQMC values. Previous work has shown that the energy and other correlations agree well. [10,36,37] We have verified that the energy in DQMC and CPQMC techniques remains in relatively good agreement in these disordered systems if the trivial difference in interaction energy is accounted for by defining,

$$E_{\text{CPQMC}}^{\text{rn}} = E_{\text{CPQMC}} + (U_{\text{DQMC}} - U_{\text{CPQMC}})(D - \frac{1}{4}). \quad (10)$$

Comparisons of the energy in CPQMC and DQMC techniques behave as shown in Fig. 15. For the parameters used in our simulations, the energies disagree by at most 5%.

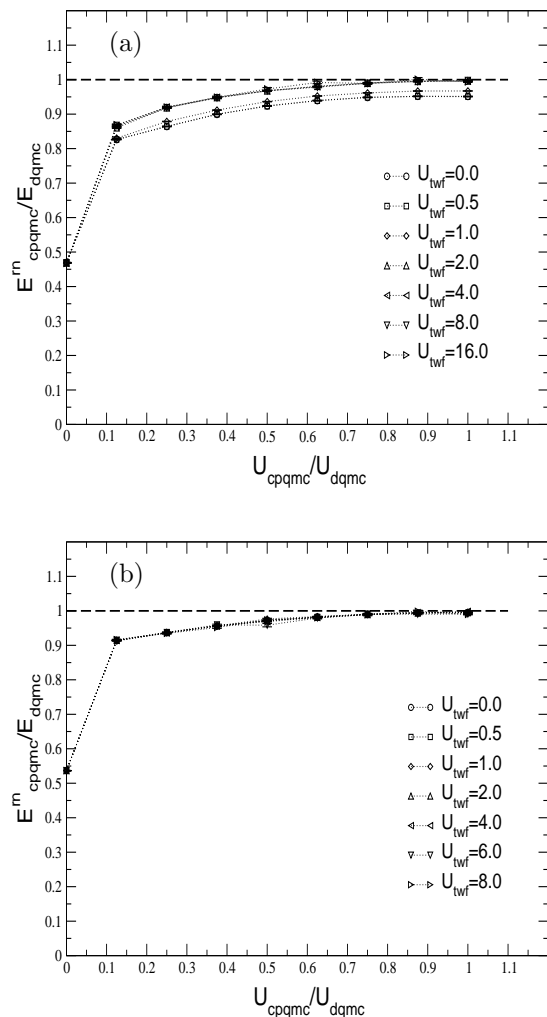


FIG. 15. Scaled data for the renormalized energy for the disordered Hubbard model in the CPQMC method: (a) 4×4 , $V_s = 2$; (b) 4×4 , $V_t = 2$.

* Present address: Department of Physics, University of Waterloo, 200 University Avenue, Waterloo, Ontario, N2L-3G1, Canada.

- [1] P. A. Lee and T. V. Ramakrishnan, *Rev. Mod. Phys.* **57**, 287 (1985), and references cited therein.
- [2] D. Belitz and T. R. Kirkpatrick, *Rev. Mod. Phys.* **66**, 261, (1994), and references cited therein.
- [3] M. Milovanović, S. Sachdev, and R. N. Bhatt, *Phys. Rev. Lett.* **63**, 82 (1989).
- [4] (a) D.B. Haviland, Y.Liu, and A.M. Goldman, *Phys. Rev. Lett.* **62** 2180, (1989); A.E. White, R.C. Dynes, and J.P. Garno, *Phys. Rev. B* **33**, 3549 (1986); (b) A.F. Hebard and M.A. Paalanen, *Phys. Rev. Lett.* **65**, 927 (1990); and (c) J.M. Valles, R.C. Dynes, and J.P. Garno,

Phys. Rev. Lett. **69**, 3567 (1992); (d) A. Yazdani and A. Kapitulnik, *Phys. Rev. Lett.* **74**, 3037 (1995).

- [5] M.P.A. Fisher, P.B. Weichman, G. Grinstein, and D.S. Fisher, *Phys. Rev. B* **40**, 546 (1989). N. Trivedi, R.T. Scalettar, and M. Randeria, *Phys. Rev. B* **54**, 3756 (1996); and R.T. Scalettar, N. Trivedi, C. Huscroft, and M. Randeria, *Phys. Rev. B* **59**, 4364 (1999).
- [6] S. V. Kravchenko, G. V. Kravchenko, J. E. Furneaux, V. M. Pudalov, and M. D'Iorio, *Phys. Rev. B* **50**, 8039 (1994), S. V. Kravchenko, W. E. Mason, G. E. Bowker, J. E. Furneaux, V. M. Pudalov, and M. D'Iorio, *Phys. Rev. B* **51**, 7038 (1995), S. V. Kravchenko, D. Simonian, M. P. Sarachik, W. Mason, and J. E. Furneaux, *Phys. Rev. Lett.* **77**, 4938 (1996).
- [7] R. Blankenbecler, R.L. Sugar, and D.J. Scalapino, *Phys. Rev. D* **24**, 2278 (1981).
- [8] S.R. White, D.J. Scalapino, R.L. Sugar, E.Y. Loh, Jr., J.E. Gubernatis, and R.T. Scalettar, *Phys. Rev. B* **40**, 506 (1989).
- [9] E.Y. Loh, J.E. Gubernatis, R.T. Scalettar, S.R. White, D.J. Scalapino, and R.L. Sugar, *Phys. Rev. B* **41**, 9301 (1990); S. Sorella, S. Baroni, R. Car, and M. Parrinello, *Europhys. Lett.* **8**, 663 (1989).
- [10] S. Zhang, J. Carlson, and J.E. Gubernatis, *Phys. Rev. Lett.* **74**, 3652 (1995); *Phys. Rev. B* **55**, 7464 (1997).
- [11] J.E. Hirsch and S. Tang, *Phys. Rev. Lett.* **62**, 591 (1989). The demonstration of long-range order in the large U Heisenberg limit is contained in J.D. Reger and A.P. Young, *Phys. Rev. B* **37**, 5978 (1988).
- [12] M. Ulmke and R.T. Scalettar, *Phys. Rev. B* **55**, 4149 (1997).
- [13] J. E. Hirsch, *Phys. Rev. B* **31**, 4403 (1985).
- [14] A yet more general MF treatment would start with a spin-rotationally invariant Heisenberg form for the interaction, and is needed, for example to capture the fact that $T_{\text{Néel}} = 0$ for the 2D model as required by the Mermin-Wagner theorem. However, since our focus is on ground state properties we have followed the example of others (Ref. [16]) and focused on the simpler decoupling, which breaks rotational invariance.
- [15] Z.G. Yu, J. Zang, J.T. Gammel, and A.R. Bishop, *Phys. Rev. B* **57**, 3241 (1998).
- [16] M. A. Tusch and D. E. Logan, *Phys. Rev. B* **48**, 14 843 (1993).
- [17] V.J. Emery, S.A. Kivelson, and H.Q. Lin, *Phys. Rev. Lett.* **64**, 475 (1990).
- [18] J. Zaanen and O. Gunnarsson, *Phys. Rev. B* **40**, 7391 (1989).
- [19] S.R. White and D.J. Scalapino, *Phys. Rev. B* **61**, 6320 (2000).
- [20] J.A. Vergis, E. Louis, P. S. Lomdahl, F. Guinea, and A. R. Bishop, *Phys. Rev. B* **43**, 6099 (1991).
- [21] C. Dasgupta and J.W. Halley, *Phys. Rev. B* **47**, 1126 (1993).
- [22] Still, it is not completely clear why MFT should be sensitive to the dimensionality. Perhaps the explanation lies in the special features (perfect nesting, logarithmic divergence of the density of states) of the clean, non-interacting band structure in two dimensions.
- [23] See, for example, K. Binder and P. Young, *Rev. Mod.*

- Phys. **58**, 801 (1986).
- [24] The enhancement in the staggered magnetization (Fig. 1) at small bond disorder and small $U = 1.0$ and 1.5 has been observed before (Ref. [12]) and explained by the enhancement of the Heisenberg exchange with disorder.
- [25] J.B. Anderson, J. Chem. Phys. **63**, 1499 (1975).
- [26] D.M. Ceperley and B.J. Alder, Phys. Rev. Lett. **45**, 566 (1980).
- [27] The mixed estimator for the energy in the CPQMC algorithm is not variational [J. Carlson, J.E. Gubernatis, G. Ortiz, and S. Zhang, Phys. Rev. B **59**, 12 788 (1999)]; however, experience has shown that the mixed estimator is almost always above the exact ground state answer in the Hubbard model.
- [28] D.A. Huse, Phys. Rev. B **37**, 2380 (1988).
- [29] S. Sachdev and N. Read and R. Oppermann, Phys. Rev. B **52**, 10286 (1995); R. Oppermann and B. Rosenow, Phys. Rev. B **60**, 10325 (1999), and references cited therein.
- [30] The extraction of the chemical potential in canonical ensemble simulations can be done using the technique described by G.G. Batrouni, R.T. Scalettar, and G.T. Zimanyi, Phys. Rev. Lett. **65**, 1765 (1990).
- [31] Measurements of the compressibility in disordered systems within dynamical mean field theory are shown by M. Ulmke, V. Janiš, and D. Vollhardt, Phys. Rev. B **51**, 10 411 (1995).
- [32] The structure factor of the bond-disordered model is relatively insensitive to U_{TWF} . Increasing U_{TWF} leads to larger fluctuations in the walker population and to a tendency for the persistence of a small staggered magnetization out to large V_i . Because of their lower population fluctuations, we believe the results for small U_{TWF} are the more reliable ones. One way around this problem would be to adjust the values of the renormalized interaction downward in simulations with large U_{TWF} . Indeed, in Fig. 14 we observe a more sensitive dependence of the renormalized interaction on U_{TWF} and V_i in larger systems.
- [33] M. Vekic, J.W. Cannon, D.J. Scalapino, R.T. Scalettar, and R.L. Sugar, Phys. Rev. Lett. **74**, 2367 (1995).
- [34] M. Ulmke, P. J. H. Denteneer, V. Janis, R. T. Scalettar, A. Singh, D. Vollhardt, and G. T. Zimanyi, Adv. Solid State Phys., **38**, 369 (1999); and references cited therein.
- [35] P.J.H. Denteneer, R.T. Scalettar, and N. Trivedi, Phys. Rev. Lett. **83**, 4610 (1999).
- [36] S. Zhang, J. Carlson, and J.E. Gubernatis, Phys. Rev. Lett. **78**, 4486 (1997); M. Guerrero, J.E. Gubernatis, and S. Zhang, Phys. Rev. B **57**, 11 980 (1998); M. Guerrero, G. Ortiz, and J.E. Gubernatis, Phys. Rev. B **59**, 1706 (1999).
- [37] C.D. Batista, J. Bonča, and J.E. Gubernatis, condmat/0009128 (unpublished).
- [38] We note that the CPQMC code works at fixed particle number and $T = 0$, while the DQMC code we used was grand canonical and finite T . To obtain ground state properties in DQMC we ran at different, decreasing T until the observables converged.
- [39] N. Bulut, D.J. Scalapino, and S.R. White, Phys. Rev. B **47** 2742 (1993); L. Chen, C. Bourbonnais, T. Li, and A.-M.S. Tremblay, Phys. Rev. Lett. **66**, 369 (1991).
- [40] J.D. Reger and A.P. Young, Phys. Rev. B **37**, 5978 (1988).